Time Evolution of Terahertz Electromagnetic Waves from Undoped GaAs/*n*-type GaAs Epitaxial Layer Structures Clarified with Use of a Time-Partitioning Fourier Transform Method

H. Takeuchi, S. Tsuruta, H. Yamada, M. Hata, M. Nakayama

SURE: Osaka City University Repository

https://dlisv03.media.osaka-cu.ac.jp/il/meta_pub/G0000438repository

The 2011 International Conference on
Luminescence and Optical Spectroscopy of Condensed Matter

Time evolution of terahertz electromagnetic waves from undoped GaAs/*n*-type GaAs epitaxial layer structures clarified with use of a time-partitioning Fourier transform method

H. Takeuchi[a,*], S. Tsuruta[b], H. Yamada[c], M. Hata[c], M. Nakayama[b]

aDepartment of Electronic Systems Engineering, School of Engineering, The University of Shiga Prefecture, 2500 Hassaka-cho, Hikone, Shiga 522-8533, Japan
bDepartment of Applied Physics, Graduate School of Engineering, Osaka City University, 3-3-138 Sugimoto, Sumiyoshi-ku, Osaka 558-8585, Japan
cTsukuba Research Laboratory, Sumitomo Chemical Co., Ltd., 6 Kitahara, Tsukuba, Ibaraki 300-3294, Japan

Abstract

We have investigated the time evolution of terahertz electromagnetic waves caused by the surge current of photogenerated carriers, the so-called first burst, in two *i*-GaAs/*n*-GaAs epitaxial layer structures with different *i*-GaAs layer thicknesses of 500 and 1200 nm. The terahertz waveform of the first burst shows a narrowing with a decrease in the thickness of the *i*-GaAs layer. In accordance with the above phenomena, it is observed in the Fourier power spectra that the band of the first burst shows a high frequency shift with a decrease in the *i*-GaAs layer thickness. We elucidate the origin of the high frequency shift, focusing on the time-domain dynamics of the photogenerated carriers: we apply the time-partitioning Fourier transform, which is useful to investigate the time evolution of the frequency. From the time-partitioning Fourier power spectra, we obtain the evidence that the acceleration after the carrier generation dominates the time evolution of the frequency component leading to the high frequency shift.

PACS: 78.47.-p; 78.47.J-; 78.66.Fd

Keywords: Ultrafast phenomena; Terahertz electromagnetic wave; Photogenerated carrier transport; Time-partitioning Fourier transform; GaAs

1. Introduction

Terahertz electromagnetic waves have been attracting much attention [1-3]. One of the reasons is attributed to the fact that the terahertz wave is a useful probe for the vibrations of biological molecules. For example, Upadhya *et al*.[4,5] investigated the inter- and intra-molecular vibrational modes of polycrystalline saccharides. They reported that the terahertz-wave absorption spectra are highly sensitive to the structure and spatial arrangement of molecules;

---

*Corresponding author. Tel.: +81-749-28-9553; fax: +81-749-28-9578.
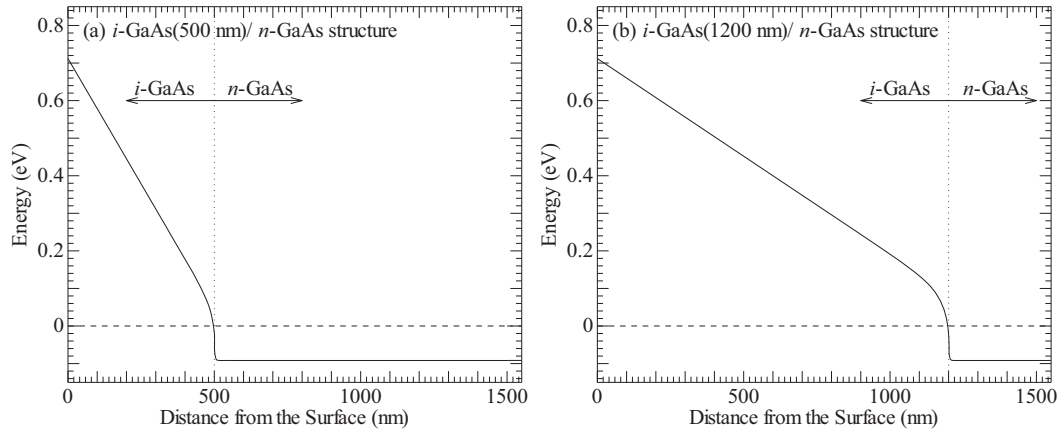*E-mail address*: takeuchi.h@e.usp.ac.jp

Fig. 1. Potential energy of *i*-GaAs(*d* nm)/*n*-GaAs epitaxial layer structure as a function of distance from the surface calculated on the basis of the Boltzmann-Poisson model. The solid and dashed lines indicate the conduction-band energy and Fermi level, respectively. (a) *d* = 500 nm. (b) *d* = 1200 nm.

namely, terahertz-wave spectrometry has the ability to discriminate each structural isomer. In terahertz-wave spectroscopy, the following two methods have been forming a mainstream. One is the method with use of a traditional Fourier-transform infrared spectrometer. The other utilizes a femtosecond pulse-laser system. In the latter method, the illumination of the pump-beam pulse onto given materials and/or photoconductive antennas, the so-called emitters, induces the terahertz waves. We note that the above-mentioned work by Upadhya *et al*. employed the latter method.

It is well known that pump-probe transient reflection and/or transmittance spectroscopic measurements, which are also based on the femtosecond laser technology, are applicable to investigate the dynamics of the vibrational phenomena in the time domain [6]. Accordingly, in principle, the femtosecond-pulse-laser-based terahertz-wave spectroscopic measurements also have the capability to investigate the transient change in the vibrational phenomena directly in the time domain. The terahertz-wave time-domain transient spectroscopic measurements, however, have been hardly carried out. The major reason arises from the lack of the information on the characteristics of the terahertz wave in the time domain, *e.g.*, the time evolution of the frequency component.

In the present work, we have investigated the time evolution of the terahertz wave from undoped GaAs (*d* nm)/*n*-type GaAs [*i*-GaAs (*d* nm)/*n*-GaAs] epitaxial layer structures, where *d* denotes the thickness of the *i*-GaAs layer: 500 and 1200 nm. We focus our attention on the following terahertz wave, the so-called first burst, which originates from the surge current of the photogenerated carriers by the pump-beam illumination. The pulse width of the first burst of the *i*-GaAs (500 nm)/*n*-GaAs structure is narrower than that of the *i*-GaAs (1200 nm)/*n*-GaAs structure. In the Fourier transform power spectra, the first burst band of the *i*-GaAs (500 nm)/*n*-GaAs structure locates at the higher frequency side in comparison with that of the *i*-GaAs (1200 nm)/*n*-GaAs structure. Using a time-partitioning Fourier transform method, we analyze the time evolution of the first burst and discuss the origin of the high frequency shift from the viewpoint of the acceleration of the carriers after the impulsive photogeneration.

2. Samples and experimental procedure

The samples were *i*-GaAs(*d* nm)/*n*-GaAs epitaxial layer structures grown on (001)-oriented semi-insulating GaAs substrates by metal organic vapor phase epitaxy. The values of *d* were 500 and 1200 nm. The doping concentration and thickness of the *n*-GaAs layer were 3×10^{18} cm^{-3} and 3 μm, respectively. The sheet resistances of the two samples were the same value of 3.1 Ω per square, which indicates that the doping process was well controlled. In order to explain the suitability of the samples to the present experiment, the calculated potential structures of the *i*-GaAs (500 nm)/*n*-GaAs and *i*-GaAs (1200 nm)/*n*-GaAs structures are shown in Figs. 1(a) and 1(b), respectively. The present calculation was performed using a computational simulation on the basis of the Boltzmann-Poisson model [7,8]. The parameter employed were the same of those used in Ref. 9. It should be noted that the surface Fermi level of *i*-GaAs locates at almost the center of the band gap [9,10]. In Figs. 1(a) and 1(b), the solid line denotes the con-
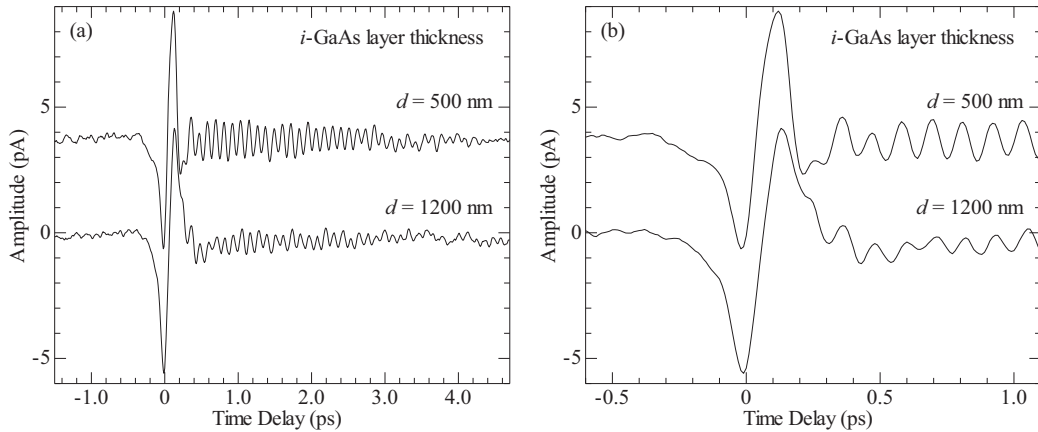
Figure 2. Amplitudes of the terahertz waveforms of the *i*-GaAs(*d* nm)/*n*-GaAs structures as a function of time delay at room temperature. (a) Terahertz waveforms in the time-delay range from -1.0 to 4.5 ps. (b) Terahertz waveforms in the time-delay range from -0.5 to 1.0 ps

duction-band energy as a function of distance from the surface, where the origin of the energy axis corresponds to the Fermi level (dashed line). The conduction-band energy has a finite linear potential slope in the *i*-GaAs layer induced by the surface Fermi-level pinning. The resultant phenomenon produces a uniform built-in electric field. The built-in electric field accelerates the photogenerated carriers and causes the surge current. Comparing Fig. 1(a) with Fig. 1(b), it is evident that the potential slope increases with a decrease in *d*, which means the built-in electric field in the *i*-GaAs layer can be controlled by *d*. The above-mentioned controllability in the built-in electric field of the *i*-GaAs layer, which dominates the acceleration process of photogenerated carriers, demonstrates the suitability of the samples to the present experiment. The values of the built-in electric field are calculated to be 13 and 5.2 kV/cm for the *i*-GaAs(500 nm)/*n*-GaAs and *i*-GaAs(1200 nm)/*n*-GaAs structures, respectively.

The time-domain terahertz-wave signals were measured using laser pulses with a duration time of ~70 fs. The pump beam was focused on the sample with the angle of incidence of 45°. The diameter of the spot on the sample surface was ~100 μm. The emitted terahertz wave was collected with use of two off-axis parabolic mirrors, and was detected by an optically gated dipole antenna with a gap of 6.0 μm formed on a low-temperature-grown GaAs layer. The powers of the pump and gate beams were fixed to 40 and 10 mW, respectively. The repetition of the laser pulses was 90 MHz. The photon energies of both the beams were the same value of 1.57 eV. The scan range of the time delay was from -2.0 to 8.0 ps. All the measurements were performed at room temperature. The humidity was kept at ~10 % during the measurement by purging with dry nitrogen gas.

3. Experimental results and discussion

Figure 2(a) shows the terahertz waveforms of the two samples. Both the samples exhibit a monocycle oscillation pulse around the time delay of 0 ps, the so-called first burst resulting from the surge current. The monocycle pulse of the first burst is followed by the long oscillation pattern with a period of 113 fs. This period corresponds to the frequency of 8.8 THz, which is the same value of the frequency of the GaAs longitudinal optical (LO) phonon. The long oscillation pattern is, therefore, assigned to the coherent GaAs LO phonon. The detailed discussion on the terahertz wave from the coherent GaAs LO phonon, which includes the generation mechanism and high emission efficiency together with the decay time, has been described in Refs. 11 and 12. In the present paper, we focus the discussion on the first burst signal. In order to highlight the pulse shape of the first burst, the terahertz waveforms between -0.5 and 1.0 ps are depicted in Fig. 2(b). It is apparent that the pulse width of the first burst signal of the *i*-GaAs(500 nm)/*n*-GaAs structure is narrower than that of the *i*-GaAs(1200 nm)/*n*-GaAs structure. In order to analyze the frequency component, we applied the Fourier transform to the terahertz waveforms. The Fourier power spectra are shown in Fig. 3. In the present Fourier transform, the time window was set to be the same as the scan range: from -2.0 to 8.0 ps. The first burst band of the *i*-GaAs(500 nm)/*n*-GaAs structure has a peak frequency at 3.2 THz, whereas that of the *i*-GaAs(1200 nm)/*n*-GaAs structure has a peak frequency 1.8 THz; namely, the first burst band shows the high frequency shift in the *i*-GaAs(500 nm)/*n*-GaAs structure. Note that, as shown in Figs 1(a) and 1(b),
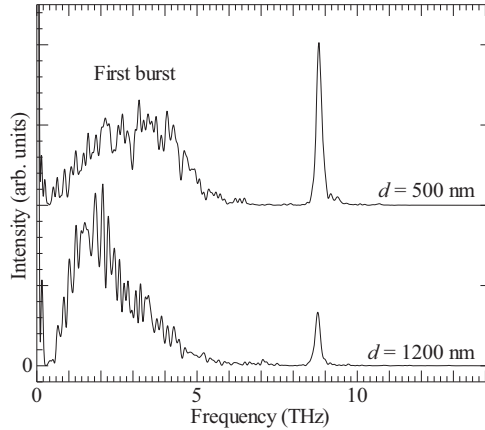
Figure 3. Fourier power spectra of the terahertz waveforms of the *i*-GaAs(*d* nm)/*n*-GaAs structures. The time window is the same as the scan range: [-2.0 ps, 8.0 ps]. The band peaking at 8.8 THz originates from the coherent GaAs LO phonon.
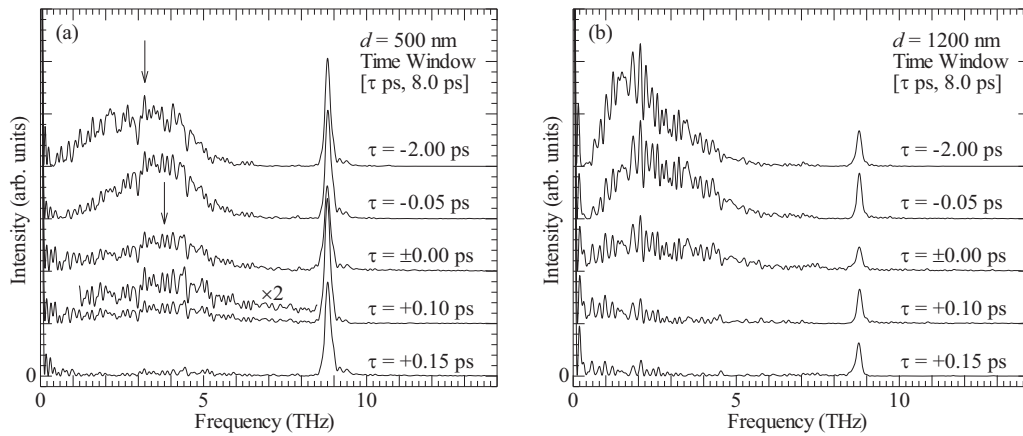

Figure 4. Time-partitioning Fourier power spectra of the *i*-GaAs(*d* nm)/*n*-GaAs structures. (a) *d* = 500 nm. (b) *d* = 1200 nm.

the built-in electric field in the *i*-GaAs layer of the *i*-GaAs(500 nm)/*n*-GaAs structure is higher than that of the *i*-GaAs(1200 nm)/*n*-GaAs structure. This fact means that the *i*-GaAs(500 nm)/*n*-GaAs structure has the high ability to accelerate the photogenerated carriers in comparison with the *i*-GaAs(1200 nm)/*n*-GaAs structure. Accordingly, the following mechanism can be assigned to a responsible factor for the frequency shift shown in Fig. 3: the acceleration of the photogenerated carriers after the pump-beam illumination. This is because, in general, the acceleration of the carriers and/or current leads to the high frequency shift of the emitted electromagnetic wave with respect of time. We note that the above-mentioned scenario is analogous to the operation principle of high frequency electronic devices.

In order to verify the above-mentioned consideration, we performed the time-partitioning Fourier transform [13]. The time-partitioning Fourier power spectrum $I(\omega)$, where ω is a frequency, is given by the following equation:

$$I(\omega) \propto \left| \int_{\tau}^{8\,ps} A(t)\exp(-i\omega t)dt \right|^2 .$$

(1)

Here, $A(t)$ is the terahertz waveform and τ is the time delay (-2 ps $\leq \tau <$ 8 ps) determining the time window of the time-partitioning Fourier transform. We note that the time-partitioning Fourier transform has been applied to investigate the time evolution and decay time of the coherent LO phonon and LO-phonon-plasmon coupled mode [14-16].

The time-partitioning Fourier power spectrum of each sample is shown in Figs. 4(a) and 4(b). In the *i*-GaAs(500 nm)/*n*-GaAs structure, the peak frequency shifts to the high frequency side with an increase in *τ*. Consequently, the high frequency shift is attributed to the carrier acceleration after the impulsive photogeneration. We also note that, in the *i*-GaAs(1200 nm)/*n*-GaAs structure, the peak frequency hardly shifts as shown in Fig. 4(b). This is because the built-in electric field, which accelerates the carriers, is much smaller in the *i*-GaAs(1200 nm)/*n*-GaAs structure than that in the *i*-GaAs(500 nm)/*n*-GaAs structure. Thus, we conclude that the carrier acceleration plays a main role for the time evolution of the first burst in the terahertz wave.

Finally, we compare the present results with those of the Monte Carlo simulation. According to the Monte Carlo simulation [17], the transient electron velocity in a GaAs crystal is accelerated by an electric field and reaches the maximum value of 5.5×10^7 cm/s at 0.5 ps in the condition of the electric field of 10 kV/cm. In the electric field of 5.0 kV/cm, the transient time of ~1 ps, which is longer than the duration time of the pulse of the first burst as shown in Fig. 2(b), is required to reach the maximum electron velocity. In addition, the maximum electron velocity in the electric field of 5.0 kV/cm is 3.5×10^7 cm/s, which is slower than the maximum electron velocity in the electric field of 10 kV/cm. From the above simulation, it is apparent that the acceleration of the electron is much smaller in the electric field of 5.0 kV/cm than that in the electric field of 10 kV/cm. The above-mentioned simulation result coincides with the present experimental result that, in the *i*-GaAs(1200 nm)/*n*-GaAs structure, the peak frequency hardly shifts in comparison with the *i*-GaAs(500 nm)/*n*-GaAs structure as shown in Fig. 4(b). Taking account of the above discussion, we conclude that the present experimental results are reasonable.

The above-mentioned conclusion is supported by the earlier work by Abe *et al*. [18]. They compared the electron velocity estimated from the terahertz-wave measurement with that calculated with use of an ensemble Monte Carlo method. The above-mentioned comparison shows a good agreement. This agreement suggests that the frequency of the terahertz wave is dominated by the electron velocity. Accordingly, their report supports the appropriateness of the present conclusion that the time evolution of the terahertz-wave frequency connects with the transient carrier velocity.

4. Summary

We have investigated the time evolution of the terahertz wave induced by the surge current of the photogenerated carriers in the *i*-GaAs(500 nm)/*n*-GaAs and *i*-GaAs(1200 nm)/*n*-GaAs epitaxial structures. From the Fourier power spectra of the terahertz waves induced by the surge current, it has been found that the first burst band of the *i*-GaAs(500 nm)/*n*-GaAs structure has a relatively high peak frequency in comparison with the result of the *i*-GaAs(1200 nm)/*n*-GaAs structure. In order to investigate the transient property of the surge current, we have applied the time-partitioning Fourier transform method in order to analyze the time evolution of the terahertz-wave frequency because the generation of the terahertz wave connects with the surge current. It has been elucidated that, in the *i*-GaAs(500 nm)/*n*-GaAs structure, the peak frequency considerably shifts to the high frequency side with an increase in the time delay. We, therefore, conclude that the carrier acceleration after the impulsive photogeneration dominates both the time evolution and the frequency component of the terahertz wave.

To finalize the present paper, we point out that the improvement of the present time-partitioning Fourier transform method, for example, the appropriate choice of the window function, leads to the step up to terahertz-wave time-domain transient spectroscopy.

References

[1] For a review, P. H. Bolivar, Coherent Terahertz Spectroscopy. In Semiconductor Quantum Optoelectronics, A. Miller, M Ebrahimzadeh, and D.M Finlayson (eds.) Chapter 5, Institute of Physics, Bristol, 1999.

[2] For a review, K. Sakai (ed.) *Terahertz Optelectronics*, Springer, Berlin, 2004.

[3] For a review, H. Takeuchi, Terahertz Electromagnetic Waves from Semiconductor Epitaxial Layer Structures: Small Energy Phenomena with a Large Amount of Information. In: *Wave Propagation*, A. Petrin (ed.), Chapter 6, INTECH, Vienna, 2011.

[4] P. C. Upadhya, Y. C. Shen, A. G. Davies, and E. H. Linfield, J. Biol. Phys. 29 (2003) 117.

[5] P. C. Upadhya, Y. C. Shen, A. G. Davies, and E. H. Linfield, Vib. Spectrosc. 35 (2004) 139.

[6] For a review, T. Dekorsy, G. C. Cho, and H. Kurz, Coherent Phonons in Condensed Media. In: *Light Scattering in Solids VIII*, M. Cardona and G. Güntherodt (eds.), Chapter 4, Springer, Berlin, 2000.

[7] P. A. Basore, IEEE Trans. Electron. Devices 37 (1990) 337.

[8] D .A. Clugston and P. A. Basore, PC1D version 5: 32-bit solar cell modeling on personal computers. In: *Proceedings of the 26th IEEE Photovoltaic Specialists Conference*, pp. 207-210, IEEE, Piscataway, NJ, 1998.

[9] H. Takeuchi, Y. Kamo, Y. Yamamoto, T. Oku, M. Totsuka, and M. Nakayama, J. Appl. Phys. 97 (2005) 063708.

[10] H. Shen, M. Dutta, L. Foiadis, P. G. Newman, R. P. Moerkirk, W. H. Chang, and R. N. Sacks, Appl. Phys. Lett. 57 (1990) 2118.

[11] H. Takeuchi, J. Yanagisawa, S. Tsuruta, H. Yamada, M. Hata, and M. Nakayama, Jpn. J. Appl. Phys. 49 (2010) 082001.

[12] H. Takeuchi, J. Yanagisawa, S. Tsuruta, H. Yamada, M. Hata, and M. Nakayama, Phys. Status Solidi C 8, (2011) 343.

[13] D. Gabor, J. IEEE 93 (1946) 429-457.

[14] M. Hase, K. Mizoguchi, H. Harima, F. Miyamaru, S. Nakashima, R. Fukasawa, M. Tani, and K. Sakai, J. Lumin. 76&77 (1998) 68-71.

[15] M. Hase, S. Nakashima, K. Mizoguchi, H. Harima, and K. Sakai, Phys. Rev. B 60 (1999) 16526.

[16] H. Takeuchi, K. Mizoguchi, M. Nakayama, K. Kuroyanagi, T. Aida, M. Nakajima, and H. Harima, J. Phys. Soc. Jpn. 70 (2001) 2598.

[17] K. Tomizawa, *Numerical Simulation of Submicron Semiconductor Devices*, Chapter 5, Artech House, Boston, MA, 1993.

[18] M. Abe, S. Madhavi, Y. Shimada, Y. Otsuka, and K. Hirakawa, and K. Tomizawa, Appl. Phys. Lett. 81 (2002) 679.

Time Evolution of Terahertz Electromagnetic Waves from Undoped GaAs/*n*-type GaAs Epitaxial Layer Structures Clarified with Use of a Time-Partitioning Fourier Transform Method

H. Takeuchi, S. Tsuruta, H. Yamada, M. Hata, M. Nakayama

Self-Archiving by Author(s)

Placed on: Osaka City University Repository